InSAR Observations and Insights into Aleutian Volcanism

7

For our study of Aleutian volcanoes we processed nearly 12,000 SAR images acquired by ERS-1, JERS-1, ERS-2, Radarsat-1, Envisat, ALOS, and TerraSAR-X from the early 1990s to 2010. We combined those images to produce about 25,000 interferograms, which we analyzed for evidence of surface deformation at each of the arc's historically active volcanoes. Where the evidence was sufficient, we used analytical source models to constrain the location, shape, and volume change of each probable deformation source that we could identify. We concluded that magmatic, hydrothermal, tectonic, and thermoelastic (cooling) processes all play a role in causing surface deformation at Aleutian volcanoes. We tried to identify a dominant deformation mechanism in each case, recognizing that the available data are inherently ambiguous. By combining our InSAR results with information from the geologic record, historical eruption accounts, seismology, petrology, gas geochemistry, and other sources, we developed conceptual models for the magma plumbing systems and behavior of as many volcanoes as possible. We realize that these models are simplistic, but it is our hope that they will serve as starting points for more thorough studies as additional information becomes available. In this chapter we summarize our findings and identify a few key research topics that seem especially ripe for additional study.

7.1 Deformation of Aleutian Volcanoes is Common and Deformation Styles are Diverse

Our InSAR study of the volcanoes of the Aleutian arc led us to some expected findings and a few surprising ones. In the latter category are the discoveries that Aleutian volcanoes are even more dynamic than their recent eruptive histories indicate, and that so much of their activity is amenable to study with InSAR. Among the 52 historically active volcanoes that we investigated, only 12 (Segula, Little Sitkin, Great Sitkin, Carlisle, Kagamil, Vsevidof, Gilbert, Shishaldin, Dutton, Pavlof, Chiginagak, Ukinrek Maars) showed no evidence of surface deformation of any kind during the period of observation. Included on that list are two volcanoes (Shishaldin, and Pavlof) that erupt repeatedly without deforming (see Sect. 7.1.1). For another eight volcanoes (Kasatochi, Bogoslof, Amak, Griggs, Mount Katmai, Snowy Mountain, Kukak, and Wrangell), decorrelation or poor spatial resolution prevented us from obtaining any useful information from the InSAR observations (Kasatochi erupted in 2008 and Bogoslof erupted in 1992) (Fig. 7.1). We found evidence of at least one episode of magma intrusion beneath 21 of the volcanoes we examined (Tanaga, Akta, Korovin, Seguam, Recheshnoi, Okmok, Makushin, Akutan, Westdahl, Kupreanof, Veniaminof, Ugashik-Peulik, Martin, Mageik, Trident, Fourpeaked, Douglas, Augustine, Iliamna, Reboubt, Spurr), plus the Strandline Lake area north of Mount Spurr. So more than 80 % of the volcanoes we studied either deformed in some way (including deformation of young flows, see Sect. 7.1.5) or erupted since the early 1990s. Magma intruded the crust beneath nearly 60 % of them.[1] We observed shallow-seated subsidence that we attribute to contraction of lava flows or pyroclastic deposits, or to hydrothermal processes, at 11 of 44 volcanoes (25 %) for which we have useful observations. In addition, we observed deeper-seated deflation that we attribute to magma reservoirs beneath the Fisher, Emmons Lake, and Aniakchak calderas. During the same ~20-year period, 17 of the 52 volcanoes we examined (33 %) erupted at least once (http://avo.alaska.edu/volcanoes/).

[1] In some cases we grouped two or more vents together because they are close enough to one another to be included in a single SAR image (e.g., the Katmai volcanic cluster (Mount Martin, Mount Mageik, Trident Volcano, Mount Katmai, Novarupta, Mount Griggs) plus Snowy Mountain and Kukak Volcano). As a result, Chap. 6 comprises 38 sections that collectively address the 52 vents included in our study. To calculate the percentages listed in this chapter, we treated each vent separately. So, for example, the percentage of volcanoes that deformed or erupted during the study period is:

$$\frac{52(total) - 12(no\ deformation) + 3(no\ deformation, erupted) - 8(no\ useful\ observations) + 2(no\ useful\ observations, erupted)}{52(total) - 8(no\ useful\ observations)} = 84\,\%$$

Similarly, the percentage of volcanoes that experienced intrusions or erupted is:

$$\frac{21(inferred\ intrusions) + 3(no\ deformation, erupted) + 2(no\ useful\ observations, erupted)}{52(total) - 8(no\ useful\ observations)} = 59\,\%$$

Z. Lu and D. Dzurisin, *InSAR Imaging of Aleutian Volcanoes*,
Springer Praxis Books, DOI: 10.1007/978-3-642-00348-6_7,

This is a high level of activity compared to most other volcanic arcs on the planet. For example, only one eruption has occurred in the Cascade arc since the 1990s (Mount St. Helens, 2004–2008) (Scott et al. 2008), while one other intrusive event is inferred to have occurred at the Three Sisters volcanic center (1997–present) (Dzurisin et al. 2009).[2] Those two sites make up 16 % of the 12 large volcanic centers in the Cascades. Among those 12, 4 (33 %) are known to have deformed since the 1990s: Mount St. Helens (eruption), Three Sisters (uplift), Medicine Lake Volcano (subsidence) (Poland et al. 2006), and the Lassen volcanic center near Lassen Peak (subsidence) (Poland et al. 2004). Both arcs are considerably more active than was recognized a few decades ago, thanks in large part to expanded ground-based monitoring networks and the advent of satellite remote sensing for the detection of ash clouds, volcanic gas plumes, and ground deformation. Later in this chapter we compare the level of activity in the Aleutians with that in two other arcs that have been well studied with InSAR: the Andean arc in South America and the West Sunda arc in Indonesia.

Also impressive and somewhat surprising is the fact that so much of the volcanic activity in the Aleutians—a region noted for snow and ice cover, locally dense tundra vegetation, rapid surface change, and notoriously bad weather—is amenable to study with InSAR. InSAR has proven to be a remarkably robust tool for mapping surface deformation and surface changes in the Aleutians, including volcanic lava flows, volcaniclastic deposits, and tephra deposits. Advanced InSAR data processing techniques, notably MTInSAR (PSInSAR, SBAS InSAR), and MAI, have extended the technique's reach to areas with few coherent targets or severe atmospheric artifacts, thus providing deformation time series that would not be available otherwise.

In addition to being nearly ubiquitous, deformation is remarkably diverse at Aleutian volcanoes (Fig. 7.1). Diversity is manifest as both spatial variations in deformation patterns among various volcanoes and as temporal changes in deformation behavior at individual volcanoes. This probably reflects the fact that Aleutian volcanoes span a broad range of eruptive styles, sizes, magma compositions, and local tectonic settings (e.g., along-arc variability in strain, crustal thickness, etc.). Differing deformation patterns suggest differences in magma plumbing systems as well. For example, 100-km-long Unimak Island hosts three historically active volcanoes: Westdahl, Fisher Caldera, and Shishaldin. In terms of eruption frequency, Shishaldin is the most active among the group and Fisher is the least active. Our InSAR analysis indicates that a magma reservoir about 6 km BSL beneath Westdahl Peak has been inflating continuously, albeit at a declining rate, since the most recent eruption in 1991–1992. Shishaldin erupts more often than Westdahl, so one might expect more deformation at Shishaldin as well. On the contrary, our InSAR results show that little or no deformation occurred at Shishaldin before, during, or after eruptions in 1995–1996, 1999, and 2004 (see Sect. 7.1.1). Deformation at Fisher differs from that observed at either Westdahl or Shishaldin. Unlike the others, Fisher is subsiding steadily at a rate of 1–2 cm/year. Even though these three volcanoes are only about 20 km apart, their deformation behaviors are remarkably different. The same is true for many adjacent volcanoes along the arc.

7.1.1 Open-Conduit Volcanoes can Erupt Without Deforming

One very clear and not very surprising result of our study is that some Aleutian volcanoes erupt without deforming appreciably (Cleveland, Shishaldin, and Pavlof), and others deform appreciably without erupting (Akutan and Ugashik-Mount Peulik are prime examples). In the first category are mafic stratovolcanoes that erupt frequently and produce local volcanic earthquakes, but seemingly without major disturbance to the surrounding crust. Following the 2004 eruption at Shishaldin, Neal et al. (2005) wrote:

> Since its last eruption in 1999, the background level of seismic activity at this frequently active volcano has remained relatively high.… Typically, this activity is interpreted to reflect either hydrothermal or magmatic processes occurring high in the conduit and deep in the summit crater of Shishaldin (Caplan-Auerbach and Petersen 2005).

Our InSAR observations revealed no evidence of surface deformation at Shishaldin, Cleveland, or Pavlof, even though the observations span at least two eruptions in each case. We concur that background seismicity at Shishaldin is indicative of processes occurring in the conduit and crater, rather than in the surrounding crust. The situation is similar at Pavlof, where frequent eruptions are accompanied by even lower levels of seismicity with very few VT earthquakes. A long list of volcanoes outside the Aleutian arc (not all mafic centers) that fit into this category of eruptions without deformation includes Aracar, Copahue, Galeras,

[2] Crider et al. (2008, 2011) attributed increased thermal activity and magmatic gas emission at Mount Baker in 1975, which was followed by a substantial gravity increase and slight deflation of the edifice, to magma intrusion at mid-crustal levels or opening of a conduit for release of magmatic volatiles. That event pre-dates the earliest InSAR observations and therefore we did not include it in our tabulation of activity in the Cascades for comparison to the Aleutians. The only other documented activity at Cascade volcanoes during historical time (excluding normal hydrothermal activity) are eruptions at Mount St. Helens during 1800–1857 and 1980–1986, and at Lassen Peak during 1914–1917.

(a)
Kasatochi:
No useful information due to coherence loss.
2 km
Atka Volcanic Center:
persistent subsidence plus uplift episode (2006 seismic swarm and eruption); d = 2–3 km (subsidence) and 4–7 km (uplift); hydrothermal system cooling/fluid loss plus magma intrusions.
Kanaga:
persistent subsidence; surficial; lava flow contraction.
Great Sitkin:
no deformation.
Gareloi:
persistent subsidence; surficial; flow contraction; no eruption-related deformation (1996).
Tanaga:
uplift episode and seismic swarm (2005); d = 3–8 km; magma intrusion.
Little Sitkin:
No deformation.
Semisopochnoi (Cerberus):
persistent subsidence; surficial; flow contraction.
Kiska:
episodic uplift and subsidence; d = 0 km; hydrothermal p/d.
Segula:
No deformation.
Amlia
Fracture Zone
Kiska
Segula
Little Sitkin
Semisopochnoi
Gareloi
Tanaga
Kanaga
Great Sitkin
Kasatochi
Atka Volcanic Center

(b)
Seguam:
persistent subsidence (western caldera) plus alternating u/s (eastern caldera); d = 2 km (both sources, subsidence) and d = 3–5 km (eastern source, uplift); magma cooling /degassing (subsidence) plus episodic magma intrusion (uplift).
Amukta:
persistent subsidence; d= 0–1 km; lava flow contraction and magma cooling/degassing.
Yunaska:
persistent subsidence; surficial; lava flow contraction.
Cleveland:
persistent subsidence; surficial; lava flow contraction; no eruption-related deformation (open-vent system).
Vsevidof/Recheshnoi:
persistent uplift plus localized subsidence; d= 4-6 km (uplift); magma intrusion and hydrothermal cooling/degassing.
Okmok:
uplift/subsidence episodes plus persistent subsidence; d = 2–3 km (u/s) plus surficial; episodic magma intrusion/withdrawal plus time-decaying lava flow contraction.
Makushin:
persistent subsidence plus uplift episode (1993–95); d =7 km (u/s); magma or hydrothermal cooling /degassing (subsidence) plus magma intrusion (uplift).
Akutan:
persistent uplift plus 1996 u/s episode (volcano flanks) plus persistent subsidence (caldera); d = 5–7 km (persistent uplift plus u/s episode, d = 0–1 km (caldera subsidence); steady magma accumulation (uplift) plus 1996 dike intrusion (u/s) plus hydrothermal cooling /degassing (subsidence, caldera).
Westdahl:
time-decaying uplift episodes plus co-eruptive subsidence; d = 6 km (u/s); magma accumulation and withdrawal.
Fisher:
persistent subsidence; d = 5–7 km; magma or hydrothermal cooling/degassing.
Shishaldin:
no eruption-related deformation (open-vent system).
Carlisle:
No deformation.
Amlia Fracture Zone
Seguam
Amukta
Yunaska
Carlisle
Cleveland
Okmok
Vsevidof
Recheshnoi
Makushin
Akutan
Westdahl
Fisher
Shishaldin

(c)
Chiginagak:
No deformation.
Veniaminof:
steady uplift; d = 6 km; magma accumulation.
Aniakchak:
persistent subsidence; d = 3–4 km; magma or hydrothermal cooling/degassing.
Kupreanof:
persistent subsidence plus uplift episode (2002–03); d = 3–6 km (subsidence) and 4–6 km (uplift); magma cooling/degassing (subsidence) plus magma intrusion (uplift).
Dutton, Emmons Lake Volcanic Center:
no deformation at Dutton, persistent subsidence (caldera), no eruption-related deformation (Pavlof); d = 7 km (subsidence); magma or hydrothermal cooling /degassing plus open-vent system (Pavlof).
Becharof Discontinuity
Chiginagak
Aniakchak
Veniaminof
Kupreanof
Emmons Lake Volcanic Center
Dutton

◀ **Fig. 7.1** Interpretative summary of InSAR results for Aleutian volcanoes: **a** western section from Kiska Volcano to the Atka volcanic center, **b** west-central section from Seguam to Shishaldin, **c** east-central section from Frosty to Chiginagak, **d** eastern section from Peulik to Spurr. Model source depths are relative to sea level and rounded to the nearest kilometer. The text refers to type of surface displacement, depth, and inferred cause. p/d, pressurization/depressurization; u/s, uplift/subsidence. "flow contraction" refers to surficial deposits including lava flows, pyroclastic flows, or tephra. "no deformation" means none observed during period of InSAR observations, which varies from a few years to nearly two decades. Deformation is not found at Kagmil and Gilbert, and no useful InSAR information can be obtained for Bogoslof, Amak or Wrangell. Horizontal scale bars represent 5 km unless stated otherwise. Landsat image mosaic of the Aleutian arc courtesy of Steve Smith of AVO/UAF

Irrupuntuncu, Lascar, Nevado del Chillan, Ojos del Salado, Reventador, Sabancaya, Ubinas, and Villarica in the Andes (Pritchard and Simons 2002, 2004a, b, c; Fournier et al. 2010; Ebmeier et al. 2010), Dempo and Merapi in west Sunda (Chaussard and Amelung 2012), and Bezymianny, Kliuchevskoi, and Sheveluch in Kamchatka, Russia (Pritchard and Simons 2004c; Lundgren and Lu 2006).

Several plausible explanations for eruptions without deformation have been proposed (Moran et al. 2006). One is that any pre-eruptive inflation is balanced continually by a similar amount of co-eruptive deflation, resulting in little or no net deformation if the InSAR image brackets both the inflation and deformation periods. A second possibility is that magma reservoirs at these volcanoes are deep enough that any inflation or deflation causes only broad, subtle deformation of the surface that is difficult to detect. Alternatively, the reservoirs might be so shallow that surface deformation does not extend beyond a small area near the summit. Such deformation would be especially difficult to detect with InSAR if coherence were lost owing to perennial ice or snow high on the volcano. A fourth plausible explanation for the lack of observed deformation at many frequently active volcanoes is that they are "open-conduit" systems where magma can reach the surface from a variety of reservoir geometries with relative ease without appreciably deforming the surrounding crust.[3]

All three frequently-active Aleutian volcanoes mentioned above (Shishaldin, Cleveland, Pavlof) are located in the central part of the Aleutian arc between the Amlia fracture zone (AFZ) to the west (Geist et al. 1987) and the Becharof discontinuity (BD) to the east (Decker et al. 2008) (Fig. 4.12).[4] Buurman et al. (2014) identified those features as important in controlling seismicity along the arc and pointed out that, in the central part of the arc: (1) erupted products tend to be lower in SiO_2 content, (2) with few exceptions, seismicity extends to greater depths beneath individual volcanoes than in the eastern or western parts of the arc, and (3) a large proportion of earthquakes deeper than about 10 km are low-frequency events indicative of fluid movement—probably magma ascent (Fig. 7.2). Buurman et al. (2014) attributed relatively deep, low-frequency earthquakes to magma flux through the lower crust and offered two end-member scenarios to explain its greater vigor in the central part of the arc. In the first scenario, the magma production rate is uniform throughout the entire arc and magma ascent is choked off near the ends by tectonic circumstances that differ from those in the central part (i.e., highly oblique subduction in the west, increased compression in the east owing to collision of the buoyant Yakutat block with the North American plate). In the second scenario, the magma production rate varies along the arc as a function of the amount of water being subducted into the mantle to initiate flux melting. Water is transported into the mantle in sediments riding on the subducting plate or in serpentinized crust that is prevalent along fracture zones. Buurman et al. (2014) explained how, in either case, the magma production rate is expected to be higher in the central part of the arc than near the ends. In the first case, the AFZ is a bathymetric high that acts as a barrier to westward transport of sediment, most of which comes from turbidites sourced in the Alaska Range far to the east. Consequently, sediment thickness increases from east to west along the central part of the arc until it decreases abruptly west of the AFZ (Scholl et al. 1982; Singer et al. 2007). In the second case, two important sources of serpentinized crust subducting into the mantle along the Aleutian trench are the AFZ and the Aja fracture zone beneath the Gulf of Alaska (Naugler and Wageman 1973) (see Fig. 4.12). As a consequence of the subduction-zone geometry, the AFZ migrates to the west over time and the

[3] The descriptor "open-conduit" is used here to refer to volcanoes that erupt frequently or for long periods of time without appreciable ground deformation except possibly very near the vent. The eruption frequency at an open-conduit volcano is such that it is able to keep the conduit hot and ductile based on thermal state and rate of infilling. The term does not imply the existence of a continuous magma-filled conduit from a kilometers-deep source to the surface. Such a conduit might exist in some cases such as the current situation at the summit of Kīlauea volcano, Hawai'i, where a vent that opened in March 2008 is occupied by a persistent lava lake. In such cases the term "open-vent," implying that the magma column is exposed continuously to the atmosphere, seems more appropriate.

[4] Other authors have applied the descriptors western, central, and eastern to different segments of the Aleutian arc. For example, Miller and Smith (1987) defined the Eastern Aleutian arc as that portion built entirely on continental crust, and the western arc as the portion built on oceanic crust. For our purposes and for reasons that we explain later in this chapter, we use the term "central Aleutian arc" or "central Aleutians" to refer to the section of arc between the Amlia fault zone on the west and the Becharof discontinuity on the east. In our nomenclature, the western Aleutian arc (Western Aleutians) is the part west of the Amlia fracture zone and the eastern Aleutian arc is the part east of the Becharof discontinuity.

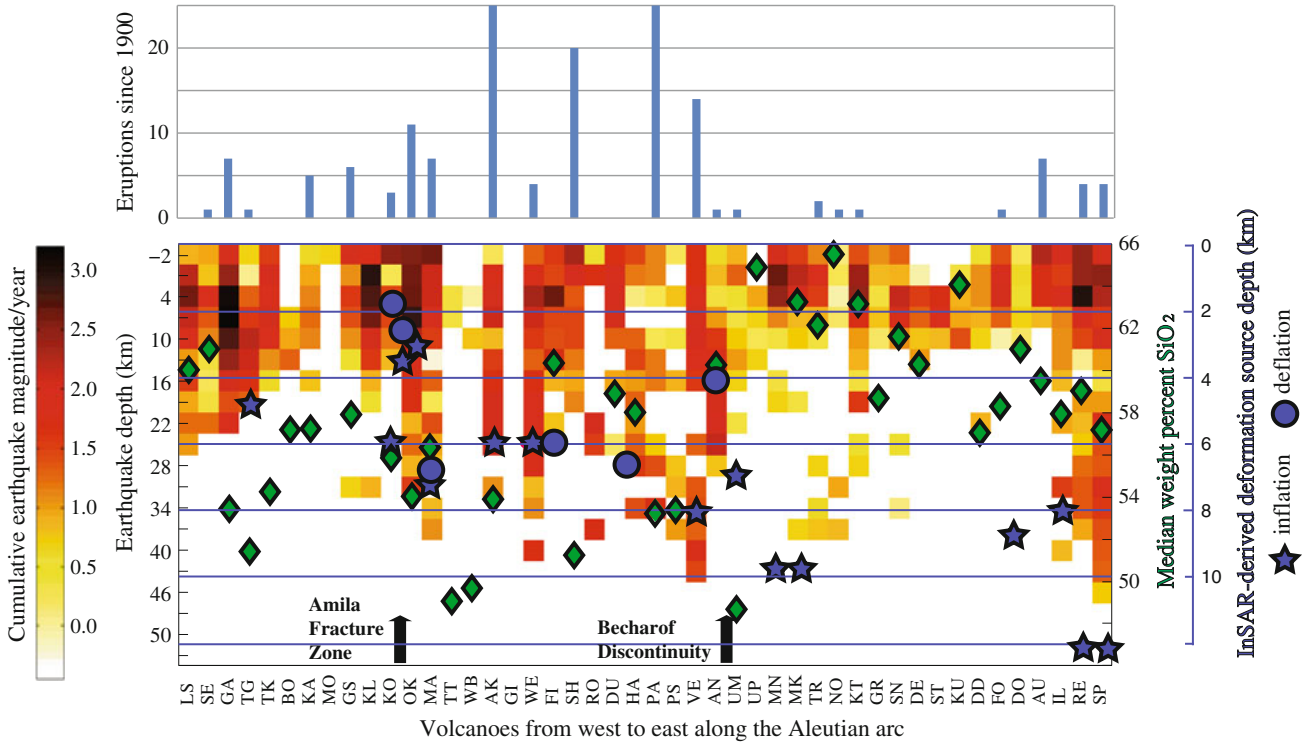

Fig. 7.2 (*top*) Number of confirmed eruptions since 1900 along the Aleutian arc (http://avo.alaska.edu/searches/eruptsearchresults.php?fromsearch=1&yearstart=1900&yearend=2010&year=&volcano=-1); (*bottom*) Comparison of average magma composition (*green diamonds*) (Nye 2008), seismicity distribution (*squares*) (Buurman et al. 2012), deformation source depths (*blue star* for inflation and *blue circle* for deflation) (this study). The *color legend* on the *left* is for the distribution of cumulative earthquake magnitude per year of data within 3-km-depth bin below each Volcano (Thelen et al. 2010). Volcano codes: *LS*, Little Sitkin; *SE*, Semisopochnoi; *GA*, Gareloi; *TG*, Tanaga; *TK*, Takawangha; *BO*, Bobrof; *KA*, Kanaga; *MO*, Moffett; *GS*, Great Sitkin; *KO*, Korovin; *KL*, Kliuchef; *OK*, Okmok; *MA*, Makushin; *TT*, Table Top; *WB*, Wide Bay; *AK*, Akutan; *GI*, Gilbert; *WE*, Westdahl; *FI*, Fisher; *SH*, Shishaldin; *RO*, Roundtop; *DU*, Dutton; *HA*, Hague; *PA*, Pavlof; *PS*, Pavlof Sister; *VE*, Veniaminof; *AN*, Aniakchak; *UM*, Ukinrek Maars; *UP*, Ugashik-Peulik; *MA*, Martin; *MK*, Mageik; *TR*, Trident; *NO*, Novarupta; *KT*, Katmai; *GR*, Griggs; *SN*, Snowy; *DE*, Denison; *ST*, Steller; *KU*, Kukak; *DD*, Devil's Desk; *FO*, Fourpeaked; *DO*, Douglas; *AU*, Augustine; *IL*, Iliamna; *RE*, Redoubt; *SP*, Spurr

Aja migrates to the east.[5] In the past, their sweep across the central part of the arc would have delivered water-rich serpentine to the mantle, facilitating magma production there relative to the western and eastern parts of the arc, where less water was subducted.

Regardless of which factor is more important (i.e., stress regime or subducted water content), magmatism is more vigorous in the central part of the arc than in the western or eastern parts. Following the lead of Buurman et al. (2014), we envision the central Aleutians as a place where the magma production rate is relatively high and/or where mafic magma can ascend through the crust relatively quickly and easily. As a result, Cleveland, Shishaldin, and Pavlof are open-conduit systems where eruptions occur frequently without much surface deformation. For volcanoes of this type, further advances in our understanding from the perspective of deformation monitoring require (1) better temporal sampling than is available from current SAR satellites, and (2) a long-wavelength and short-repeat sensor to reduce interferometric decorrelation due to persistent snow/ice cover. As shown during the 2006 eruption at Augustine (Cervelli et al. 2010), adequate monitoring of such volcanoes also requires data from dense networks of CGPS stations (some of which should be as close to the vent as possible) and seismometers to capture any localized or short-term deformation that might occur (see Chap. 6, Augustine Sect. 6.35). In addition, adequate gas measurements are important to monitor open-conduit systems. Furthermore, petrologic studies of eruption products, and 3-D geophysics and subsurface imaging can also provide key constraints.

[5] Features on the subducting Pacific plate west of the arc's midpoint (i.e., the point where convergence is orthogonal) migrate westward along the arcuate Aleutian trench over time, while points east of the midpoint migrate eastward. So the AFZ migrates westward while the BD and Aja fracture zone migrate eastward. As a result, their locations relative to volcanoes along the arc change over long time scales.

We recognize that factors other than crustal stress differences play a role in influencing volcanic activity along the arc (e.g., crustal composition, subducted sediment flux), and also that interactions among several factors undoubtedly complicate the situation (e.g., local tectonic setting, magma composition, melt production and ascent rate, crustal residence time, etc.). Nonetheless, the interpretive framework proposed by Buurman et al. (2014) is generally consistent with our InSAR results and we believe it provides a useful context for the discussion that follows.

7.1.2 Many Volcanoes Deform Without Erupting

Akutan is an instructive counterexample to the open-conduit systems discussed above. Like Shishaldin, Cleveland, and Pavlof, Akutan is located in the central part of the Aleutian arc and it erupts frequently—16 times from 1962 to 1992. What sets Akutan apart from its open-conduit neighbors is an intense swarm of earthquakes that occurred during March 1996, which (1) included more than 200 events larger than magnitude 3.5, (2) produced a zone of ground cracks up to 500 m wide and more than 3 km long, (3) was accompanied by intrusion of a dike to within a few hundred meters of the surface…but did not culminate in an eruption. Why? It seems likely that the March 1996 event was both magmatic and tectonic in nature, the latter component evidenced by formation of graben structures with vertical displacements of 30–80 cm and by reactivation of Holocene normal faults on the island (see Akutan Sect. 6.21). Comparable features have been absent during all recent eruptions at Shishaldin, Cleveland, and Pavlof, where activity has been dominantly magmatic in nature and seismicity has been much less intense. We include Akutan in a category of volcanoes where magmatism and tectonism are linked in such a way that a predominantly tectonic event sometimes triggers a magmatic response or vice versa.

Another instructive example of an Aleutian volcano deforming without erupting, also with a tectonic subplot to the story, is what happened at Ugashik-Mount Peulik and Becharof Lake, 30 km to the northwest, during 1996–1998. Recall from Sect. 6.32 that Mount Peulik inflated more than 20 cm during that period without erupting, and that the inflation episode was followed by an intense swarm of earthquakes beneath Becharof Lake. The only reports of eruptions at Mount Peulik, both of which are regarded as questionable, were in 1814 and 1852. One possibility, of course, is that the inflation episode and seismic swarm were unrelated except, coincidentally, by their timing. We think this is unlikely, especially in light of the fact that another swarm beneath Becharof Lake accompanied formation of the Ukinrek Maars, 15 km to the southeast, in 1977. Although the magmas erupted at Ukinrek and Mount Peulik are chemically distinct and any direct link between their plumbing systems is unlikely, they seem to share a tectonic connection as expressed by seismicity beneath Becharof Lake.

Why did Mount Peulik not erupt during 1996–1998 in response to magma accumulation beneath it and a strong regional earthquake swarm, whereas other Aleutian volcanoes erupt frequently without inflating and with much less seismic energy release? We can think of four factors that might have played a role. First, Peulik had not erupted in more than 150 years, so the formation of an eruptive conduit would have required more work than at volcanoes that erupt more frequently. Second, the erupted products at Peulik are a calcalkaline suite of basalt, andesite, dacite, and rhyolite, ranging in SiO_2 content from 51 to 72 %. Magmas erupted at Shishaldin, Cleveland, and Pavlof are generally more mafic, ranging from basalt to basaltic andesite. Any silicic magma bodies that might exist beneath Peulik could impede the ascent of magma from greater depth, resulting in reservoir inflation but not an eruption. Third, Peulik is located on the rim of the Ugashik caldera, whereas Shishaldin and Cleveland are not associated with caldera systems and Pavlof sits a few kilometers outside the rim of the Emmons Lake caldera. Perhaps the magmatic plumbing systems of Mount Peulik and the Ugashik caldera are linked more directly than is the case for Pavlof Volcano and the Emmons Lake caldera. Fourth and perhaps most importantly, Ugashik-Peulik sits at the intersection of the Ugashik Lakes fault system, the Bruin Bay fault, and the Becharof discontinuity (Decker et al. 2008). Buurman et al. (2014) have shown that marked changes in magma composition and volcano seismicity occur across the BD. In the central part of the arc to the west, erupted magmas tend to be lower in SiO_2 content, seismicity extends to greater depths, and a large proportion of earthquakes deeper than 10 km are low-frequency events indicative of fluid movement. Mount Peulik shows an affinity for a group of volcanoes east of the BD where SiO_2 contents are greater, deep earthquakes are much less common, and low-frequency events are rare. In fact, the background level of seismicity of any kind at Peulik is very low, with only a few locatable events per year. We speculate in a later section that these characteristics of volcanism east of the BD are indicative of lower magma production rates at present, longer magma residence times in the crust, and added compressive stress across the arc—all relative to the central part of the arc and all of which tend to inhibit eruptive activity. These factors combined with the unusual structural complexity of the Ugashik-Peulik area might help to explain why Mount Peulik did not erupt during the 1996–1998 swarm and inferred intrusion. Shishaldin, Cleveland, and Pavlof, on the other hand, are located in the central part of the arc where we think

primary magma production rates are higher and crustal residence times are shorter—factors that favor frequent eruptions of more primitive magmas over non-eruptive intrusions and evolution of more silicic magmas.

7.1.3 A Deep Deformation Source Near a Volcano is Not Synonymous with Magma, but…

We attribute most cases of broad surface uplift (e.g., Tanaga, Atka volcanic center, Seguam, Okmok, Makushin, Akutan, Westdahl, Kupreanof, Veniaminof, Peulik, Katmai volcanic cluster, Fourpeaked, Iliamna, Spurr, and Strandline Lake) to magma intrusion, in part because most of the model sources are located at or below 5 km BSL. This is deeper than hydrothermal fluids are thought to exist in active volcanic environments (Fournier 2007). On the other hand, we acknowledge that a deep model source is not synonymous with magma. Our numerical and conceptual models are simplistic and non-unique. Magmatic systems are inherently complicated, involving physical and chemical interactions among tectonic strain, magma (itself a complex three-phase mixture of melt, crystals, and gas), groundwater, and heterogeneous host rock (Dzurisin 2007; Segall 2010). A broad deformation signal that is well-fit by a single deep point source of dilatation can be equally well fit by a large array of shallow sources of varying strength. Faced with such ambiguity in the cause(s) of broad surface uplift, we generally resort to the Occam's razor principle and favor what we perceive to be the simplest explanation, i.e., magma intrusion.

We also realize that surface uplift can be caused by pressurization of a magma reservoir without additional input of magma (Dzurisin 2007). This is perhaps the strongest argument for making simultaneous geodetic and precise gravity measurements at volcanoes—the only technique capable of detecting subsurface mass changes and thus distinguishing between new magma influx (net increase in mass) and pressurization by volatiles trapped in a preexisting magma body (no net change in mass) (Gottsmann and Rymer 2002; Battaglia et al. 2008).

In the absence of supporting geophysical or geochemical evidence, our presumption of magma intrusion as the cause of observed surface uplift at many Aleutian volcanoes is open to question. Nonetheless, the frequent occurrence of precursory uplift at volcanoes that eventually erupt and then subside in a similar pattern is strong circumstantial evidence for the existence of magma reservoirs that are supplied and replenished by intrusions from below, and which occasionally feed intrusions toward the surface.

7.1.4 Caldera Systems are Especially Dynamic

Another observation from our study that was not surprising is that large caldera systems in the Aleutians tend to deform a lot. Newhall and Dzurisin (1988) came to that conclusion based on their compilation of caldera unrest around the world. Miller and Smith (1987) listed 12 volcanic centers in the eastern Aleutian arc where one or more caldera-forming eruptions have occurred during Late Pleistocene or Holocene time: Okmok, Makushin, Akutan, Fisher, Emmons Lake, Aniakchak, Black Peak, Veniaminof, Ugashik, Katmai, Novarupta, and Kaguyak. The Black Peak and Kaguyak calderas are relatively small (3 and 2.6 km diameter, respectively) and neither has erupted for about a millennium (Siebert et al. 2010). We found evidence of recent deformation at all 10 of the other young calderas. Since 1992 when InSAR observations began, eruptions have occurred at Okmok (1997, 2008), Makushin (1993, 1995), Akutan (1992), and Veniaminof (several). Uplift that we ascribe to magma accumulation in the upper crust has occurred at all four of those sites. Three of the four (excluding Veniaminof) also have experienced either persistent or episodic subsidence that we attribute to magma or hydrothermal system cooling and degassing, or to episodic magma withdrawal. Persistent subsidence also is occurring at Semisopochnoi, Atka, Seguam, Yunaska, Fisher, Emmons Lake, and Aniakchak. These results leave little doubt that the floors of calderas underlain by partly molten or still hot magma bodies, which can persist for hundreds of thousands of years, tend to be mobile. At such places, surface deformation is the norm rather than an exception.

7.1.5 Surface Subsidence of Various Kinds is a Common Process at Aleutian Volcanoes

We have observed three types of subsidence fields in our study of Aleutian volcanoes. The first type occurs at recent lava flows or pyroclastic flow deposits at volcanoes such as Semisopochnoi, Gareloi, Kanaga, Seguam, Amukta, Yunaska, Cleveland, Okmok, and Augustine. In general, the pattern of subsidence mimics the flow distribution and the greatest amount of subsidence occurs where the flow is thickest. We investigated several possible explanations for this type of behavior and concluded that thermoelastic contraction as a result of cooling is the most likely cause (Lu et al. 2005). In a few cases, surface loading by young flows also plays a role (see Chap. 6, Sect. 6.18.7 for details). In addition, we suspect mechanical compaction can be a significant subsidence mechanism shortly after the emplacement of volcanic

deposits. We suspect that contraction is a nearly ubiquitous feature of young volcanic deposits of all types in the Aleutians and elsewhere. Where subsidence of recent flows or domes was not observed (e.g., Redoubt, Shishaldin, Pavlof, Kasatochi), it might be (1) masked by other deformation, (2) occurring at a rate below the InSAR detection threshold, or (3) hidden by coherence loss.

Another type of subsidence was observed at Kiska Volcano, the Atka volcanic center (Korovin), Seguam, Recheshnoi, and Akutan. In these cases the subsidence fields do not correlate with the distributions of young deposits, and modeling suggests source depths in the range 0–4 km BSL. A telling observation is that subsidence of this type mostly occurs in association with notable surface hydrothermal activity. In a few cases where persistent subsidence was interrupted by an uplift episode (e.g., Makushin, Korovin), modeling suggests that the uplift source was deeper than the subsidence source. For these reasons we attribute subsidence of this type primarily to hydrothermal-system depressurization as a result of fluid loss. We did not observe subsidence at all active hydrothermal areas in the Aleutians, presumably because (1) the rate of fluid loss is low owing to self-sealing of microfractures by mineral deposition and quasi-plastic flow, or (2) alternating episodes of self-sealing (uplift) and rupturing (subsidence) produce little net surface displacement (Fournier 2007).

The third type of subsidence we observed is sourced at greater depth than the other two types, typically at 5–12 km BSL, in an area which at other times is a source of uplift. Examples include Makushin, Okmok, Fisher, Emmons Lake volcanic center, Kupreanof, and Aniakchak. Because the source locations for uplift and subsidence are essentially the same, and because some of the uplift episodes have culminated in eruptions, we attribute this third type of surface subsidence to cooling and fluid loss from crustal magma reservoirs. At systems with similar deformation behavior, but which have not erupted during historical time (e.g., the Yellowstone caldera), uplift and subsidence both might be sourced in the deep hydrothermal system rather than in the underlying magmatic system (Dzurisin et al. 2012). Numerical simulations suggest that relatively deep hydrothermal fluid flow can produce significant ground surface deformation at large calderas (Wicks et al. 1998; Fournier 2007; Hurwitz et al. 2007). However, we regard the hydrothermal scenario as less likely in most cases of this type—especially at Aleutian volcanoes where the same source seems to be responsible for uplift, subsidence, and eruptions.

7.1.6 Even "Dormant" Volcanoes Deform

Our study turned up evidence for episodic intrusions and associated seismic swarms even at a few volcanoes that have not erupted for more than a century. Three examples are Mount Recheshnoi where there are no reports of eruptions during historical time, Mount Kupreanof where there have been no eruptions during all of Holocene time, and Mount Peulik where the most recent eruption occurred about 150 years ago.[6] Long-dormant volcanoes that have experienced geodetic inflation outside the Aleutian arc include: Hualca–Hualca, Laguna de Maule, Lazufre, and Uturuncu in the central and southern Andes (Fournier et al. 2010; Pritchard and Simons 2004a, b), and Three Sisters volcanic center, central Oregon Cascades, USA (Wicks et al. 2002; Dzurisin et al. 2006, 2009). InSAR has played a pivotal role in identifying activity at these otherwise dormant volcanoes—leading us to conclude that intrusions of magma into the upper crust are considerably more common than had been realized earlier, and that many intrusions do not culminate in eruptions. Together with mapping volcano deformation with excellent spatial resolution, the recognition of intrusive events that might otherwise have gone unnoticed is among InSAR's greatest contributions to volcano science thus far.

7.1.7 Deformation Sources can be Offset from Eruptive Vents by Many Kilometers

At several Aleutian volcanoes, we observed deformation fields that were offset from associated eruptive vents by distances ranging from several kilometers to tens of kilometers. These include Tanaga, Korovin (Atka volcanic center), Seguam, Recheshnoi, Makushin, Okmok, and possibly Fourpeaked. See our discussion near the end of the Makushin section in Chap. 6 for hypotheses regarding the cause of such offsets. What we would like to add here is a caution that such offsets can cause important information about volcanic unrest to be missed if monitoring efforts are too narrowly focused. One lesson in this regard worth sharing here concerns Korovin volcano, located near the northern edge of the Atka volcanic center. When we processed a few InSAR images acquired during 1996–2000 to prospect for deformation associated with the June 1998 eruption at Korovin, we found nothing unusual. This led us to conclude that "…deformation associated with the eruption is either lacking or too small to be detected by ERS-1/ERS-2 InSAR…" (Lu et al. 2007). However, based on a comprehensive analysis of ERS-1/

[6] Terms such as "dormant" and "inactive" can be ambiguous when used to describe a volcano. Understanding the intended meaning always requires context. Their usage might be appropriate when discussing an eruptive pause of a few years duration at a volcano that typically erupts almost continuously, but not at a volcano where eruption intervals are measured in centuries or millennia. Here we use the terms informally to describe volcanoes that have not erupted for a period much longer than the time interval spanned by our study.

ERS-2 and Envisat images, we report here that the Atka volcanic center has experienced many episodes of uplift and subsidence since the 1990s. The center of deformation is offset from Korovin by about 5 km, and the observed InSAR fringes barely extend as far as Korovin itself. Such a pattern could easily be missed by a deformation monitoring network focused narrowly on Korovin, where most activity has occurred during historical time. A broader monitoring focus, in this case on the entire Atka volcanic center, is the better choice. In the case of Korovin-Kluichef, seismicity provides additional guidance: the strongest concentration of earthquakes occurs ~5 km south of Korovin, near Kluichef and the center of observed deformation.

Another case where attention to the "big picture" is advised is the broad inflation signal centered between Fourpeaked and Douglas volcanoes near the northeast end of the Alaska Peninsula (see Chap. 6, Sect. 6.34). The deformation source, presumably a magma storage zone, is likely linked to the Fourpeaked and Douglas vents and might be the source of future eruptions either at one of those centers or (less likely) at a new vent somewhere in the area.

7.1.8 Internal Deformation of Lava Flows and Pyroclastic Flows is Common and Long-Lasting

A final observation from our study is that subsidence of the surfaces of young lava flows and pyroclastic flows as a result of thermoelastic contraction, internal mechanical compaction, or loading by younger flows is more prevalent and persistent than we expected. We identified flow-related subsidence at Augustine (1986 and 2006 pyroclastic flows), Novarupta dome and adjacent ashflow tuff in the upper Valley of Ten Thousand Smokes, Okmok (1958 and 1997 lava flows), Seguam (1997 and 1992–1993 lava flows), Cleveland, Yunaska, Amutka, Kanaga, Gareloi, and Semisopochnoi (Cerberus). Additional examples might have escaped detection because they were masked by deeper-seated deformation or artifacts in the interferograms. Especially notable are the Augustine, Novarupta, and Okmok examples.

At Augustine, the subsidence rate of 2006 pyroclastic flow deposits was about 4 cm/month a few months after they were emplaced and about 1 cm/month 3 years later. Moreover, subsidence of 1986 pyroclastic flow deposits was still detectable by InSAR in 2008–2009, more than two decades after they were emplaced. The average thickness of 1986 and 2006 pyroclastic flow deposits at Augustine is about 10 m. Thicker flows undoubtedly subside faster and longer. The Novarupta lava dome and adjacent ashflow tuff in the upper part of the VTTS, for example, are still subsiding at detectable rates nearly 100 years after they were emplaced in the great eruption of 1912. The thickness of the tuff in the upper VTTS is not known, but may be as great as 250 m (Hildreth 1983).

A wealth of information about flow subsidence comes from Mount Okmok, where basalt flows extruded in 1958 were subsiding 1.5 cm/year about 35 years later, and at twice that rate soon after they were buried by similar flows in 1997. The 1997 flows themselves were subsiding at an average rate of 2 mm/day (72 cm/year) 4 months after they were extruded. These observations leave little doubt that both thermoelastic contraction and surface loading cause lava flow surfaces to subside, in some cases for many decades. Subsidence rates undoubtedly vary from case to case depending on flow thickness and the mechanical strength of the substrate, among other factors.

7.2 Episodic Intrusion: An Intrinsic Feature of Aleutian Volcanism

At several Aleutian volcanoes we have uncovered evidence of surface inflation that occurs more or less continuously (albeit at time-varying rates) for periods of a few years or longer. We interpret this behavior as a consequence of the continuous process of magma formation, ascent, storage in the crust, and (in some cases) eruption. Recheshnoi, Okmok, Westdahl, and Akutan are three examples of this type. On the other hand, a larger percentage of Aleutian volcanoes inflate only episodically. These include Tanaga, Atka volcanic center, Makushin, Kupreanof, Peulik, Iliamna, Spurr, and the Strandline Lake area (included on the basis of 1996–1998 earthquake swarm and associated surface uplift). At these sites, ground surface uplift associated with magma intrusion often is accompanied by swarm seismicity. In such cases, swarms are a good indicator of magma intrusion. In other cases (e.g., Recheshnoi, Westdahl, Akutan, Okmok, Seguam) the intrusion process is mostly aseismic.

Makushin provides an illustrative example of deformation that we attribute to episodic intrusive behavior. In the early 2000s when we processed and analyzed ERS-1/ERS-2 images that were acquired from 1992 to 1998, we discovered that Makushin had inflated as much as 7 cm during 1993–1995 (Lu et al. 2002). Because no usable SAR imagery was acquired in 1994, we could not narrow down the timing of the deformation any further. In the absence of evidence to the contrary, we associated the inflation with a small, short-lived eruption at Makushin in January 1995 and attributed it to "pre-eruptive magmatic inflation" (Lu et al. 2002). In hindsight, our confidence in that interpretation is tempered for three reasons. First, there were reports of possible eruptive activity at Makushin on September 14, September 23, and November 5, 1993, and another on January 14, 1994. The January 1995 eruption was probably somewhat larger than

those events, but the exact timing of the 1993–1995 inflation detected with InSAR relative to the reported events is not known. A second reason is that the volume of tephra erupted during the January 1995 eruption is not well known and so cannot be compared to the source volume change we estimate from InSAR (other than to say that both were small (0.02 km^3 from InSAR)). Third, we now know from InSAR observations that episodic intrusions occur frequently beneath volcanoes in the Aleutians and elsewhere. In other words, the surface inflation at Makushin that is known to have occurred sometime during 1993–1995 might not be directly associated with any one eruption and could have accumulated in more than one episode. Presumably, the 1993–1995 InSAR observations show the net effect of one or more small intrusions into a reservoir about 7 km BSL that fed each of the eruptions during that period.

We consider episodic intrusions of magma into the crust an integral part of the workings of many Aleutian volcanoes. Factors that promote the progression of magmatic intrusions into eruptions include high gas content, rapid gas exsolution, decreasing magma viscosity, and a favorable stress environment—all of which favor rapid magma ascent (Moran et al. 2011). Factors that can impede such progress include magma overpressure below some critical threshold (Pinel and Jaupart 2004), high or increasing magma viscosity, non-favorable stress environment, and the buffering effect of geothermal systems (Moran et al. 2011; Tait et al. 1989). Our InSAR results provide evidence that at least one of these factors played a role in arresting recent intrusions in the Aleutians. For example, time-series analysis of ground surface deformation at the Atka volcanic center and Peulik shows that inflation episodes there lasted from a few weeks to several months. In these two cases and others in the Aleutians, surface inflation stopped before the associated earthquake swarms ended—a behavior that seems consistent with a stalled intrusion continuing to cause seismicity while strain is accommodated in the host rock. The relatively slow pace of some intrusions and the consequent retarding effect of gas escape might be primary controls on why some intrusions do not culminate in eruptions, both in the Aleutians and elsewhere.

The 1996 earthquake swarm and surface deformation episode at Akutan is the clearest example in our study of a magmatic intrusion that approached to within a few hundred meters of the surface without erupting (Moran et al. 2011). The InSAR observations show that Akutan was uplifted at a steady rate of about 10 mm/year for several years both before and after the 1996 swarm—behavior that we attribute to slow but persistent accumulation of magma in a reservoir 5–7 km BSL. When the reservoir ruptured in March 1996, as indicated by the onset of vigorous seismicity, a dike propagated upward. Models of the surface displacement field mapped by InSAR indicate that the dike reached to within about 400 meters of the surface, probably during the height of the seismic swarm from March 11 to 15. There the dike stalled, but not before near-surface rocks were strained to the point of failure—resulting in an extensive zone of ground cracks (Power et al. 1996; Lu et al. 2000). In this case, strain accommodation by faulting probably was a factor in the dike's failure to reach the surface.

7.3 Evidence of Volcano-Tectonic Interactions

The deepest deformation sources identified in our study occur in the eastern part of the arc, beneath the northeastern part of the Alaska Peninsula and Cook Inlet region (Figs. 7.1 and 7.2). From the Ugashik-Mount Peulik volcanic center northeastward, the depths of sources that we interpret as magma reservoirs increase from about 7 km BSL at Mount Peulik to 10–14 km at Mount Spurr and 12–16 km beneath the Strandline Lake area. Source depths beneath nearby Iliamna Volcano ($d = 8$ km), Augustine Volcano ($d = 7$–12 km), and Fourpeaked Mountain ($d = 5$–10 km) are among the next deepest group, which also includes the Martin-Mageik-Trident cluster ($d = 5$–15 km). The average depth of all magma reservoirs we identified in the eastern part of the arc is about 10 km. For comparison, source depths we were able to estimate for 8 volcanoes in the central part from Aniakchak to Seguam (excluding shallow-seated deformation sources attributed to flow contraction or hydrothermal processes) are in the range 4–8 km, with an average of about 6 km. West of Seguam we were able to locate only two uplift sources that we interpret as magma reservoirs, i.e., beneath the Atka volcanic center (4–7 km BSL) and Tanaga (3–8 km BSL). These estimated source depths are similar to those for the central part of the arc but they are too few for meaningful comparison to other parts of the arc. We recognize that the small sizes of islands in the western Aleutians might have prevented us from identifying other, possibly deeper sources. We are confident, on the other hand, that deformation sources that we associate with magma storage zones are generally deeper in the eastern part of the arc than in the central part. Taken together, these observations led us to consider what factors might influence the depth of crustal magma storage along the arc, and whether our results are consistent with (1) along-arc variations in plate convergence rate, convergence angle, stress regime, or nature of the overriding plate, and (2) current ideas about arc segmentation, including the importance of major structural discontinuities along the arc.

7.3.1 Along-Arc Variations in Convergence Rate, Convergence Angle, and Downdip Velocity

The Pacific plate-North American plate convergence rate decreases from ~8 cm/year in the western part of the Aleutian arc to ~7 cm/year in the central part near Unimak Island and further to ~6 cm/year in the eastern part near Cook Inlet (DeMets 1992; Demets et al. 1994). Over the same geographic span, the convergence angle (obliquity) varies from −80° in the west to 0° in the center near Unimak Island (orthogonal convergence) to +40° in the east. As a result, the relative downdip velocity varies from ~1 cm/year in the western part to ~6 cm/year in the central part and ~4 cm/year in the eastern part. Oblique convergence near the ends of the arc introduces an element of right-lateral shear in the west and left-lateral shear in the east (Fig. 4.7).

There is no clear correspondence between variations in any of these parameters and our observation that magma reservoirs tend to be deeper in the eastern part of the arc than in the central or western parts. Instead, the change in average reservoir depth occurs in the vicinity of the BD, a northwest-trending zone of crustal weakness defined by Decker et al. (2008) that crosses the arc at Ugashik-Mount Peulik. We see no corresponding change in average reservoir depth across the AFZ to the west, but as mentioned above we were able to locate only two deep sources (inferred reservoirs) west of the AFZ.

7.3.2 Along-Arc Changes in Stress Regime

Oblique subduction has resulted in westward migration of the Aleutian forearc along right-lateral transcurrent faults (Avé Lallemant and Oldow 2000) and along-arc variations in present-day stress regime (Geist et al. 1988; Lu and Wyss 1996). To investigate any relationship between our InSAR-derived deformation sources and stress regime, we consulted the World Stress Map (Heidbach et al. 2008; Ruppert et al. 2012) and focal mechanisms for large crustal earthquakes along the Aleutian arc. The axis of maximum horizontal compressional stress is oblique to the trend of the arc west of Ugashik-Mount Peulik, and more nearly perpendicular to the arc from Ugashik-Mount Peulik northeastward to Mount Spurr (Fig. 4.12). So our results indicate that magma reservoirs tend to be deeper where regional horizontal compressional stress is greatest, i.e., northeast of the BD (Naugler and Wageman 1973; Kay et al. 1982).

7.3.3 Differences Between Oceanic and Continental Parts of the Arc

The North American plate consists of oceanic lithosphere west of Unimak Island and continental lithosphere to the east (Cooper et al. 1976; Worrall 1991; Fliedner and Klemperer 2000). There is a corresponding change in dip of the subducting slab from ~60° in the western and central parts of the arc to ~25° in the eastern part. As a result, the distance between the Aleutian megathrust and the volcanic arc increases from 150 to 200 km west of Unimak Island to more than 400 km at Mount Spurr. Other factors being equal, magma rising beneath the arc would become neutrally buoyant and pond deeper in continental lithosphere than in denser oceanic lithosphere. This is generally consistent with our observation that the deepest magma reservoirs occur in the eastern part of the arc. On the other hand, the change in average reservoir depth occurs nearly 600 km east of the oceanic-continental lithosphere boundary near Unimak Island. So any influence that lithosphere type might have on reservoir depth seems to be of secondary importance.

Another possibility is that the depth of magma storage is influenced by differences in crustal thickness along the arc. Calvert and McGeary (2013) pointed out that the Aleutian arc as a whole, with a crustal thickness estimated by various authors to be 27–35 km, has the thickest island arc crust on Earth. Near the transition from oceanic to continental arc, Calvert and McGeary (2013) identified two seismically reflective and mostly aseismic roots extending from ~25 to 50–55 km depth, which they interpreted as mafic to ultramafic bodies formed by repeated intrusion of mantle-derived melts. They noted that no similar features are evident farther west along the arc, and speculated that eventually such roots founder into the underlying mantle. The two "ultradeep roots" identified by Calvert and McGeary (2013) are considerably west of and deeper than our deepest interpreted magma reservoir (12–16 km BSL at Strandline Lake), and they are also west of the BD where we see a change in average reservoir depth. So any influence on reservoir depth of crustal thickness or the extent of intrusive roots along the arc seems weak to nonexistent.

7.3.4 Structural Influences on Magma Production Rate, Composition, and Storage

The 2,500-km-long Aleutian arc is complex at many scales and any trends we might infer from the InSAR results are vague at best. Dividing the arc into segments with common

characteristics helps to simplify the problem and develop a model for testing. Partitioning of the Aleutian arc into a small number of discrete segments has been proposed on the basis of the rupture lengths of great earthquakes (Boyd et al. 1988), inferences from structural geology (Geist et al. 1988; Ryan and Scholl 1993; Geist and Scholl 1994), differing stress orientations from seismic fault plane solutions (Lu and Wyss 1996), and geodetic measurements (Savage 1983; Kienle and Swanson 1983; Savage et al. 1986, 1999; Cross and Freymueller 2007; Fournier and Freymueller 2007). As described above, for our purposes we divide the arc into three segments. The western segment extends from Kiska Volcano eastward to the AFZ just east of the Atka volcanic center. The central segment stretches from Seguam eastward to Ugashik-Mount Peulik or, in other words, from the AFZ to the BD. The eastern segment is that portion of the arc from the BD to Mount Spurr, the northeasternmost Aleutian volcano that has erupted during historical time.

Recent studies have shown that segmentation of the arc is manifested by differences in the compositional range of erupted magmas and in the vertical extent of crustal seismicity between central and eastern segments of the arc and, to a lesser degree, between central and western segments (Nye 2008; Buurman et al. 2014). Nye (2008) presented major-element chemical data for eruptive products along the length of the arc and showed that in the eastern part of the arc andesites and dacites are the dominant magma types (Fig. 7.2). In the central segment from Chiginagak southwest to Seguam, where the AFZ intersects the arc, tholeiitic basalts and basaltic andesites are more prevalent. Farther west, from the Atka volcanic center to Kiska Volcano (western segment), calcalkaline andesites and basaltic andesites are the most common erupted products. Buurman et al. (2014) showed that seismicity generally extends to greater depths in the central part of the arc (generally >30 km) than in the western (generally <20 km) or eastern (generally <10 km) parts (Fig. 7.2). Earthquakes less than about 10 km deep along the entire arc are mostly volcano-tectonic (VT) events, whereas deeper earthquakes tend to be low-frequency (LF) events. LF events are much more common in the central part of the arc that in the western or eastern part—a pattern that Buurman et al. (2014) attributed to greater magma flux in the lower crust beneath the central Aleutians.[7] These differences in seismicity mirror the compositional differences reported by Nye (2008) and Buurman et al. (2014). In a general way they also mimic the difference between average magma storage depths in the central and eastern parts of the arc that we report here. In all three studies, the difference between the central and eastern parts of the arc is more pronounced than the difference between the central and western segments.

One factor that might influence volcano seismicity, magma composition, and depth of magma storage is magma production rate. Other factors being equal (unlikely), we would expect the production rate to mimic the downdip velocity of the subducting slab. If the water content of the slab did not vary along the arc, the amount of water available to initiate flux melting of the mantle wedge would be directly proportional to the subducting mass flux, i.e., to the downdip slab velocity. In that case, the magma production rate would be greatest in the central part of the arc, where the downdip velocity is ~6 cm/year, less in the eastern part (~4 cm/year), and least in the western part (~1 cm/year) where subduction is highly oblique. Buurman et al. (2014) made a similar but more refined argument for relatively high magma production rates in the central Aleutians, based on the flux of sediment or serpentinized crust into the mantle (see also Kay and Kay 1994; Fournelle et al. 1994; Singer et al. 2007).

As a crude proxy for magma production rate, we plotted the number of confirmed eruptions since the start of the twentieth century at each volcanic center along the arc (http://avo.alaska.edu/volcanoes/eruptsearchresults.php?fromsearch=1&yearstart=1900&yearend=2010&year=&volcano=-1) (Fig. 7.2). As expected the central part of the arc has produced the greatest number of eruptions, peaking at 20–25 at Akutan, Shishaldin, and Pavlof. Fewer eruptions have occurred in the western and eastern segments of the arc. Contrary to the ideas mentioned above, the average number of eruptions per volcano since 1900 is higher in the western segment of the arc (~2 eruptions/volcano) than in the eastern segment (~1 eruption/volcano). This in spite of the fact that the volcanoes in the eastern Aleutian arc are close to large population centers, whereas the western Aleutians are remote and eruptive activity there is more likely to be underreported. A possible explanation for the apparent discrepancy is that, at some locations in the western Aleutians, strike-slip motion and block rotation as a result of highly oblique convergence is more conducive to magma ascent than is the tectonic setting in the eastern part of the Aleutian arc (see below).

There have been notably few eruptions (0–2 per volcano) since 1900 at volcanoes in a ~200 km-long portion of the eastern arc segment from Ugashik-Peulik to Douglas. The relative paucity of eruptions in that part of the eastern arc is reminiscent of the abrupt changes in seismicity and magma composition reported by Buurman et al. (2014). We acknowledge that the number of historical eruptions is a poor proxy for magma production rate—erupted volume over a much longer time period (challenging to determine

[7] Buurman et al. (2014) noted significant deep earthquake activity below Mount Spurr and Redoubt Volcano in the eastern segment of the arc, which they regarded as exceptions to the general lack of deep seismicity there. They attributed the exceptions to recent eruptions that involved magma flux in the lower crust.

geologically) would be a better indicator—but at the same time we are intrigued by yet another example of an abrupt change near the boundary between the central and eastern parts of the arc as we define them here. Returning for the moment to the issue of magma production rate, we point out that 11 of 13 caldera-forming eruptions in the Aleutians during Late Pleistocene or Holocene time occurred in the central part of the arc: Okmok (2), Makushin, Akutan, Fisher, Emmons Lake, Aniakchak (2), Veniaminof, Black Peak, and Ugashik (Miller and Smith 1987, p. 435). This is essentially the same span of arc that has produced the greatest number of historical eruptions (Fig. 7.2). A high magma production rate is necessary to sustain a magma body in the crust long enough and large enough to produce a large caldera-forming eruption. So both the frequency of eruptions during historical time and the locations of caldera-forming eruptions during Late Quaternary time point to high magma production rates in the central part of the arc.

What other factors might account for the non-uniform distributions of seismicity, magma composition, eruption frequency, and magma storage depth along the Aleutian arc? The most striking differences in all four observables occur near the boundary between the central and eastern segments of the arc, i.e., across the BD. To the east, deep low-frequency earthquakes are much less common, erupted magmas are more silicic, there are fewer large calderas and fewer historical eruptions, and magma reservoirs tend to be deeper. Buurman et al. (2014) attributed the relative lack of deep seismicity beneath the eastern part of the arc to a diminished flux of magma through the crust relative to the more active central part. Lesser magma flux results in longer magma residence times in the crust, more fractionation and crustal assimilation, formation of more evolved magmas, and fewer eruptions. Deeper magma storage in the eastern half of the arc might be explained in part by lesser buoyancy of magma rising through continental crust there versus oceanic crust in the western half. However, some additional factor is needed to explain why the change occurs near the BD instead of at the oceanic-continental crust boundary in the North American Plate almost 600 km to the west near Unimak Island—and at essentially the same place as conspicuous changes in seismicity and magma composition.

Buurman et al. (2014) proposed that the additional factor might be increased horizontal compressive stress across the eastern segment of the arc caused by northward displacement, low-obliquity collision, flat-slab subduction and accretion of the buoyant Yakutat terrane to the North American continent beneath the Gulf of Alaska (Bruns 1983; Plafker 1983, Plafker et al. 1994a, b) (Fig. 4.12). The Yakutat terrane is either a combination of continental and oceanic crust or thickened oceanic crust (Pavlis et al. 2004); in either case it is buoyant and resists subduction (Freymueller et al. 2008; Chapman et al. 2008). The words of Naugler and Wageman (1973, p. 1580), first quoted in Chap. 4, bear repeating here:

> Assuming the rest of Alaska is rigidly attached to the North America plate, a transition of the plate boundary from one of strike-slip displacement (the Queen Charlotte Islands fault system) to one of underthrusting (the Aleutian arc subduction zone) must be occurring within the continental crust of southeastern Alaska. This results in an unstable situation in which subduction of continental crust is required in order that a narrow zone of deformation, typifying most plate boundaries, be maintained throughout the transition. Subduction of continental crust is considered by many to be physically untenable owing to its buoyancy and hyperfusible petrologic make-up (for example, Dietz and Holden 1970). Thus, to allow for the present differential motion between the Pacific plate and the North America plate, crustal shortening by internal deformation must be occurring to relieve horizontal compressive stresses and complete the plate boundary transition. This zone of compression should lie between the eastern limit of active subduction along the Aleutian trench and the system of transform faults farther east.

One need look no further than the arcuate sweep of the Alaska Range, the Chugach-St. Elias Range, and regional reverse faults such as the Bruin Bay and Castle Mountain faults for confirmation that impingement of the Yakutat terrane on North America has been, and still is, a major compressional event (see Fig. 4.12). According to Freymueller et al. (2008, p. 3): "The southern Alaska margin features a wide zone of deformation inboard of the megathrust. The most intense inboard deformation occurs in a band that extends north and west of the St. Elias Range, where the impact of the Yakutat terrane has had the greatest effect." GPS observations show that relative motion between the Yakutat block and North America results in close to 40 mm/year of shortening within the Chugach-St. Elias Range—an exceptionally high rate that is among the highest within continental crust anywhere on Earth (Fletcher and Freymueller 1999; Freymueller et al. 2008; Elliot et al. 2010). We concur with Buurman et al. (2014) that the additional compressive stress resulting from this collision is an important limiting control on magma ascent in the eastern part of the Aleutian arc, and that the BD might isolate the central part from far-field effects of the collision. From our perspective, the choking off of magma ascent by high compressive stress might help to explain the tendency for magma reservoirs to be deeper in the eastern part of the Aleutian arc than in the central or western part.

7.4 Comparisons with Other Volcanic Arcs

7.4.1 Andean Volcanic Arc, South America

Several investigators have published InSAR-based deformation surveys of the Andean volcanic arc (Pritchard and Simons 2004a, b, c; Fournier et al. 2010) or of a specific

volcano in the arc (Chaitén; Wicks et al. 2011). In the northern Andes of Ecuador, Fournier et al. (2010) mapped surface deformation associated with shallow dike intrusion beneath Tungurahua during 2006–2008, and subsidence associated with pyroclastic flows and lava flows at Reventador. In the central Andes, Pritchard and Simons (2004a) found evidence of episodic intrusions beneath three volcanic centers: Uturuncu, Bolivia; Hualca Hualca, Peru; and Lazufre, northern Chile/northwestern Argentina. They reported model-derived source depths of 12–25 km BSL at Ururuncu, 8–18 km BSL at Hualca Hualca, and 5–13 km BSL at Lazufre. Pritchard and Simons (2004a) also identified surface subsidence at Cerro Blanco caldera, Argentina, and attributed it to depressurization of a hydrothermal system at 5–10 km BSL. In the southern Andes, InSAR investigations have identified: (1) time-varying surface uplift at Laguna del Maule volcanic center along the Chile-Argentina border (source depth $d \sim 5$ km BSL) (Fournier et al. 2010); (2) uplift and subsidence episodes at Cordon Caulle, Chile ($d = 4$–7 km BSL) (Fournier et al. 2010); (3) volcanic deflation associated with the 2008 eruption at Chaitén, Chile, ($d = 8$–12 km BSL) (Wicks et al. 2011); (4) episodic inflation at Cerro Hudson, Chile ($d \sim 5$ km BSL) (Pritchard and Simons 2004b; Fournier et al. 2010); (5) subsidence associated with hydrothermal activity at Copahue, Argentina/Chile (Fournier et al. 2010); and (6) surface lava flow contraction at Longquimay, Chile (Fournier et al. 2010).

On the other hand, InSAR detected no volcano-wide deformation associated with recent eruptions at Chilean volcanoes Nevados de Chillan, Villaricca, or Llaima, which led Fournier et al. (2010) to conclude "… most deforming volcanoes are not erupting and we do not observe deformation at most of the erupting volcanoes…" This dichotomy is present but less clear in the Aleutians, where our work has shown that *some* deforming volcanoes do not erupt and *some* erupting volcanoes do not deform. Nonetheless, it is worth noting that InSAR has shown the connection between inflation and eruptions to be less direct than it seemed previously. This is probably due in part to the fact that deformation has gone unnoticed at otherwise quiescent volcanoes, where lack of a perceived threat resulted in inadequate monitoring. Other factors that might bias the InSAR results in this regard include the short period of observation (starting in the early 1990s) and long repeat times (typically months to a year), which make it possible for sporadic or short-lived deformation episodes to go unnoticed.

Another result from the studies referenced above is that inflation sources tend to be deeper under volcanoes in the central Andes than in the southern or northern Andes. We suspect this is at least in part because the crust in the central Andes is extremely thick (>70 km) and the crustal thickness decreases both to the south and to the north (Stern 2004). This observation is consistent with our results for volcanoes in the eastern, continental portion of the Aleutian arc, where deformation sources tend to be deeper than in the oceanic portion. However, we suspect that increased compressive stress resulting from collision of the Yakutat microplate with the North American plate is more important in this regard (Fig. 4.12) (see Sect. 7.3.4).

7.4.2 West Sunda Volcanic Arc, Indonesia

Using ALOS PALSAR imagery acquired from 2006 to 2009, Chaussard and Amelung (2012) surveyed the west Sunda volcanic arc, comprising the islands of Sumatra, Java, and Bali, for evidence of volcano deformation. The arc is among the most active on Earth, with 76 volcanic centers that have erupted during historical time (Simkin and Siebert 2002). Chaussard and Amelung (2012) identified inflation at Sinabung and Kerinci in Sumatra; Slamet, Lawu, and Lamongan in Java; and Agung in Bali. Surface uplift rates were 3–8 cm/year and model source depths were in the range 1–3 km below the average regional elevation (approximately 0–2 km BSL). The authors also reported subsidence at Anak Krakatau with a source depth of about 0.7 km. No deformation was detected at the 68 other historically active volcanoes in the arc. However, we suspect that more instances of volcano deformation would be discovered over a longer observation period.

Three of the six inflating volcanoes identified by Chaussard and Amelung (2012) in the west Sunda arc (Sinabung, Kerinci, and Slamet) erupted within 0.3–2.0 years after the InSAR observation period, and the other three have erupted during historical time. The authors attributed relatively frequent eruptions and shallow magma storage to the extensional and strike-slip setting of the west Sunda arc where lower confining stress allows easier ascent of magma. They concluded (Chaussard and Amelung 2012, p. 4 of 6):

> A qualitative global analysis of arc volcanoes shows that shallow reservoirs occur in extensional and strike-slip settings but not in compressional settings. The regional tectonic setting could be an explanation for the presence of reservoirs at shallow levels at volcanoes in other geodynamic settings and is consistent with observations in the East African rift (Biggs et al. 2011).

We concur with that assessment and note that the range in source depths for inflationary sources in the west Sunda arc is shallower than in the Aleutian arc (this study), which in turn is shallower than in the Andean arc (Pritchard and Simons 2004a, b, c; Fournier et al. 2010). This is consistent with the idea that shallow magma reservoirs tend to occur in extensional settings. On the other hand, our study of the Aleutian arc identified sources of inflation beneath the

Alaska Peninsula, in a compressional setting, as deep as 12–16 km. In the central Andean arc, also in a compressional setting, Pritchard and Simons (2004a) modeled inflationary sources as deep as 12–25 km BSL. Rather than being absent in compressional settings, it seems that crustal magma reservoirs tend to be deeper there. Chaussard and Amelung (2012) illustrated this fact in their figure 3, which shows the range in reservoir depths for volcanoes in extensional, transtensional, strike-slip, transcompressional, and compressional settings. Although some reservoirs deeper than 5 km occur in every type of setting, the majority and the deepest occur in compressional settings.

As discussed above, another factor that might influence the depth of magma storage beneath volcanic arcs is the type and thickness of the overriding plate along the volcanic chain. In the Aleutians, the deepest reservoirs detected in our study occur beneath the northeast part of the Alaska Peninsula and Cook Inlet region (i.e., northeastward from the Ugashik-Mount Peulik volcanic center), where the overriding plate is continental.[8] West of Unimak Island, where the overriding plate comprises relatively thin oceanic crust, magma tends to accumulate at shallower depths. Greater buoyancy of magma rising through dense oceanic crust, relative to continental crust, might play a role, because the depth of neutral buoyancy is less in oceanic crust than in continental crust. However, this idea fails to explain the existence of relatively shallow magma reservoirs beneath the section of arc from Unimak Island east to Ugashik-Mount Peulik (e.g., Aniakchak) where the overriding plate is continental.

In the west Sunda arc, oblique convergence of the Sunda and Australian plates is accommodated by strike-slip movement along the Great Sumatran fault and dip-slip movement along the Sunda megathrust. The direction of plate convergence is about normal off western Java, oblique off Sumatra, and parallel to divergent farther north (Curray 1989). The shallow range of reservoir depths reported by Chaussard and Amelung (2012) for the west Sunda arc probably reflects the combined effects of (1) rapid subduction (6.7 ± 0.7 cm/year) (Tregoning et al. 1994), which results in vigorous magmatism, and (2) a range of tectonic settings that includes strike-slip, transtensional, and extensional settings. Some of the deepest reservoirs identified with InSAR occur beneath the Andean arc, where convergence of the Nazca plate and South American plate is nearly normal and the continental crust in the Central Volcanic Zone reaches a thickness of 70 km (Stern 2004).

[8] Continental crust has an average density of about 2700 kg/m^3, which is less dense than the average density of oceanic crust (about 2900 kg/m^3). The density of magma ranges from 2180 to 2800 kg/m^3 (Bottinga and Weill 1970). Volatile-rich magma can have significantly lower bulk density.

7.4.3 Statistical Comparison of Volcano Deformation in the Aleutian, Andean, and West Sunda Arcs

Among about 97 volcanoes in the Aleutian arc that were active in the Holocene, 52 have been historically active (http://avo.alaska.edu/volcanoes/) (Miller et al. 1998; Siebert et al. 2010). Among the 52 historically active volcanoes we examined, about 33 showed evidence of uplift, subsidence, or flow deformation (Fig. 7.1). In 18 cases, we attribute uplift or subsidence with source depths greater than 4–5 km BSL to magmatic inflation or deflation. In seven other cases with source depths shallower than 4–5 km BSL, we attribute subsidence to hydrothermal-system depressurization or fluid loss. We found evidence of localized subsidence resulting from contraction or loading of surface lava flows or pyroclastic flows in eight of the areas studied.

In the northern Andean arc, about 15 of 35 volcanoes have been active during historical time. The ALOS PALSAR InSAR survey by Fournier et al. (2010) for the period 2006–2008 detected uplift caused by magma intrusion at one of these (Tungurahua) and subsidence associated flow contraction at another (Reventador). In the central Andean arc, about 17 of 69 volcanoes have been historically active and the InSAR survey by Pritchard and Simons (2004a) for the period 1992–1998 identified 4 deforming volcanoes (3 uplift, 1 subsidence). Among 63 volcanoes along the southern Andean arc, about 27 have been historically active. InSAR studies by several authors cited above, which span 1993–1999, 2002–2008, and 2007–2010, detected deformation at seven southern Andean volcanoes. The authors cited magmatic inflation and deflation, hydrothermal-system depressurization, and flow contraction as likely source mechanisms.

Of 84 volcanic centers in the west Sunda arc, about 76 have been historically active. InSAR images that span 2006–2009 identified 6 cases of uplift and one case of subsidence (Chaussard and Amelung 2012).

Taken together, these studies suggest that surface deformation is more prevalent in the Aleutian arc than in either the west Sunda or Andean arc. The comparison is by no means rigorous in a statistical sense (the Sunda and Andean arcs are less thoroughly studied with InSAR over a shorter timespan), but it confirms what was already known, i.e., if surface deformation and other forms of unrest are considered together with eruptions, the Aleutian arc is among the most active volcanic arcs in the world.

7.5 Concluding Remarks

Our work has shown that the Aleutian arc is a dynamic place where volcanoes routinely deform as a result of magmatic, tectonic, and hydrothermal processes, and also

where volcanic deposits subside for decades after emplacement as a result thermoelastic contraction. We have demonstrated that InSAR can provide important new information about the configuration and behavior of magmatic systems beneath arc volcanoes. That is not to imply, however, that we regard this report as the final word on deformation at Aleutian volcanoes. To the contrary, our study highlights how little we know about the workings of these diverse and dangerous volcanoes. The discovery of ground deformation (or lack thereof) at a given volcano using InSAR or any other geodetic technique does not necessarily result in better allocation of monitoring resources or more informed assessments of volcano hazards. We know that some volcanoes erupt without deforming and others deform without erupting. Likewise, some eruptions are preceded or accompanied by intense seismic activity or copious releases of magmatic gases, while others are not. The challenge in the Aleutians and elsewhere is to better understand why this is the case. More and better information about how volcanoes deform is surely an advantage in this endeavor, and InSAR is an important new source of such information. Complete understanding of the eruption cycle at most of Earth's volcanoes is still beyond reach, but progress toward that goal is accelerating.

With planned launches of several next-generation SAR satellites in the coming decade, data acquisitions will become more frequent, observation intervals will be shorter, and image analysis will occur more nearly in real time. Our hope is that these developments will help to usher in a time wherein magma accumulation in the middle to upper crust can be observed long before the onset of short-term precursors to an eruption. Ultimately, more widespread use of InSAR for volcano monitoring could shed light on a poorly understood but important part of the eruption cycle, i.e., the time period between eruptions when a volcano seems to be doing essentially nothing. Combining results from advanced InSAR techniques with observations from continuous GPS stations, gravimeters, strainmeters, tiltmeters, seismometers, and volcanic gas sensors will improve our ability to forecast future eruptions, thus enabling improved volcano hazard assessment and more effective eruption preparedness.

This book is intended to be a timely report that summarizes our 3-year effort to process, analyze, and interpret thousands of InSAR images along the Aleutian volcanic arc. As such, it is neither comprehensive nor final. In our attempt to be timely, we probably overlooked some instances of subtle or short-term deformation. Although we examined about 25,000 interferograms, there are still more that could be produced from archived images and from images being acquired by past and currently operational SAR sensors. We have applied advanced InSAR analysis techniques to some, but not all, of the Aleutian volcanoes—and new techniques are being developed all the time. Taking a second or third look at an area can be surprisingly productive. For example, our first look at volcanoes on the Alaska Peninsula from the Katmai volcanic cluster to Mount Spurr, using only a few images acquired by ERS-1 and ERS-2, produced nothing exciting (Lu et al. 2007). However, subsequent processing and analysis of all available SAR images for this part of the arc, as detailed in this book, produced a much different result. It turns out that the area is among the most actively deforming sections of the entire arc. Had we taken more time to analyze more images with advanced techniques, we almost surely would have discovered more and learned more—but this report would have been less timely. There is still plenty of opportunity to improve InSAR data processing techniques, image analysis procedures, and especially the interpretations reported in this book. We invite interested readers to join us in this ongoing effort, which we find challenging, rewarding, and (dare we say it?) lots of fun.

References

Avé Lallemant, H. G., & Oldow, J. S. (2000). Active displacement partitioning and arc-parallel extension of the Aleutian volcanic arc based on global positioning system geodesy and kinematic analysis. *Geology, 28*(8), 739–742.

Battaglia, M., Gottsmann, J., Carbone, D., & Fernández, J. (2008). 4D volcano gravimetry. *Geophysics*, *73*(6), WA3–WA18. doi: 10.1190/1.2977792.

Biggs, J., Bastow, I.D., Keir, D., & Lewi, E. (2011). Pulses of deformation reveal frequently recurring shallow magmatic activity beneath the Main Ethiopian Rift. *Geochemistry, Geophysics, and Geosystems (G^3)*, *12*, Q0AB10. doi: 10.1029/2011GC003662.

Bottinga, Y., & Weill, D. F. (1970). Densities of liquid silicate systems calculated from partial molar volumes of oxide components. *American Journal of Science, 269*, 169–182.

Boyd, T., Taber, J., Lerner-Lam, A., & Beavan, J. (1988). Seismic rupture and arc segmentation within the Shumagin Island seismic gap, Alaska. *Geophysical Research Letters, 15*, 201–204.

Bruns, T.R.. (1983). A model for the origin of the Yakutat Block, an accreting terrane in the Northern Gulf of Alaska. *Geology*, *11*(12), 718–721. doi: 10.1130/0091-7613(1983)11<718:MFTOOT>2.0.CO;2.

Buurman, H., West, M.E., & Cameron, C. (2012). *What controls earthquakes at Aleutian arc volcanoes*?, Abstract V21B-2777 presented at 2012 Fall Meeting, AGU, San Francisco, California, 3–7 December.

Buurman, H., Nye, C.J., West, M.E., & Cameron, C. (2014). Regional tectonic influences on Aleutian arc volcanism. *Geochemistry, Geophysics, Geosystems,* in review January 2014.

Calvert, A. J., & McGeary, S. E. (2013). Seismic reflection imaging of ultradeep roots beneath the Eastern Aleutian Island arc. *Geology, 41*, 203–206. doi:10.1130/G33683.1.

Caplan-Auerbach, J., & Petersen, T. (2005). Repeating coupled earthquakes at Shishaldin Volcano, Alaska. *Journal of Volcanology and Geothermal Research, 145*, 151–172.

Cervelli, P., Fournier, T., Freymueller, J.T., Power, J.A., Lisowski, M., & Pauk, B. (2010). The geodetic perspective on the 2006 eruption of Augustine Volcano. In J.A. Power, M.L. Coombs, M.L., & J.T. Freymueller (Eds.), *Scientific investigations of Augustine Volcano,*

Alaska, following the 2006 eruption (pp. 427–452). U.S. Geological Survey Professional Paper 1769.

Chapman, J.B., Pavlis, T., Gulick, S., Burger, A., Lowe, L., Spotila, J., Bruhn, R., Vorkink, M., Koons, P., Barker, A., Picornel, K., Ridgeway, K., Hallet, B., Jaeger, J., & McAlpin, J. (2008). Neotectonics of the Yakutat collision—Changes in deformation driven by mass redistribution. In J.T. Freymueller, P.J. Haeussler, R. Wesson, & G. Ekstrom (Eds.), *Active tectonics and seismic potential of Alaska* (Vol. 179, pp. 65–81). AGU Geophysical Monograph.

Chaussard, E., & Amelung, F. (2012). Precursory inflation of shallow magma reservoirs at West Sunda volcanoes detected by InSAR. *Geophysical Research Letters, 39*, L21311. doi:10.1029/2012GL053817.

Cooper, A. K., Scholl, D. W., & Marlow, M. S. (1976). Plate tectonic model of the evolution of the Bering Sea Basin. *Geological Society of America Bulletin, 87*, 1119–1126.

Crider, J. G., Johnsen, K. H., & Williams-Jones, G. (2008). Thirty-year gravity change at Mount Baker Volcano, Washington, USA—Extracting the signal from under the ice. *Geophysical Research Letters, 35*, L20304. doi:10.1029/2008GL034921.

Crider, J. G., Frank, D., Malone, S. D., Poland, M. P., Werner, C., & Caplan-Auerbach, J. (2011). Magma at depth—A retrospective analysis of the 1975 unrest and Mount Baker, Washington, USA. *Bulletin of Volcanology, 73*(2), 175–189. doi:10.1007/s00445-010-0441-0.

Cross, R. S., & Freymueller, J. T. (2007). Plate coupling variation and block translation in the Andreanof segment of the Aleutian arc determined by subduction zone modeling using GPS data. *Geophysical Research Letters, 34*, L06304. doi:10.1029/2006GL028970.

Curray, J.R. (1989). The Sunda arc: A model for oblique plate convergence. *Netherlands Journal of Sea Research*, *24*(2–3), 131–140. doi: 10.1016/0077-7579(89)90144-0. http://www.sciencedirect.com/science/article/pii/0077757989901440.

Decker, P.L., Reifenstuhl, A.E., & Gillis, R.J. (2008). Structural linkage of major tectonic elements in the Ugashik-Becharof Lakes region, Northeastern Alaska Peninsula. In R.R. Reifenstuhl, & P.L. Decker (Eds.), *Bristol Bay-Alaska Peninsula region, overview of 2004–2007 geologic research* (pp. 85–103). Alaska Division of Geological & Geophysical Surveys Report of Investigation 2008-1F, 1 sheet.

DeMets, C. (1992). Oblique convergence and deformation along the Kuril and Japan trenches. *Journal of Geophysical Research, 97*, 17615–17625.

DeMets, C., Gordon, R. G., Argus, D. F., & Stein, S. (1994). Effect of recent revisions to the geomagnetic reversal time scale on estimates of current plate motions. *Geophysical Research Letters, 21*, 2191–2194.

Dietz, R. S., & Holden, J. C. (1970). Reconstruction of Pangea—Breakup and dispersion of continents. Permian to present. *Journal of Geophysical Research, 75*, 4939–4956.

Dzurisin, D. (2007). *Volcano deformation—Geodetic monitoring techniques* (p. 441 p). Berlin: Springer-Praxis Books in Geophysical Sciences.

Dzurisin, D., Lisowski, L., Wicks, C.W., Poland, M.P., & Endo, E.T. (2006). Geodetic observations and modeling of magmatic inflation at the Three Sisters volcanic center, central Oregon Cascade Range, USA. *Journal of Volcanology and Geothermal Research. Special issue, The Changing Shape of Active Volcanoes*, *150*(1–3), 35–54. doi: 10.1016/j.jvolgeores.2005.07.011.

Dzurisin, D., Lisowski, M., & Wicks., C.W. (2009). Continuing inflation at Three Sisters volcanic center, central Oregon Cascade Range, USA, from GPS, leveling, and InSAR observations. *Bulletin of Volcanology*, *71*, 1091–1110. doi: 10.1007/s00445-009-0296-4.

Dzurisin, D., Wicks, C.W, & Poland, M.P. (2012). *History of surface displacements at the Yellowstone Caldera, Wyoming, from leveling surveys and InSAR observations, 1923–2008*. U.S. Geological Survey Professional Paper 1788 (68 p.) and data files. http://pubs.usgs.gov/pp/1788/.

Ebmeier, S. K., Biggs, J., Mather, T. A., Wadge, G., & Amelung, F. (2010). Steady downslope movement on the western flank of Arenal Volcano, Costa Rica. *Geochemistry, Geophysics, Geosystems, 11*, Q12004. doi:10.1029/2010GC003263.

Elliott, J.L., Larsen, C.F., Freymueller, J.T., & Motyka R.J. (2010). Tectonic block motion and glacial isostatic adjustment in Southeast Alaska and adjacent Canada constrained by GPS measurements. *Journal of Geophysical Research*, *15*, B09407. doi: 10.1029/2009JB007139.

Fletcher, H., & Freymueller, J. T. (1999). New GPS constraints on the motion of the Yakutat block. *Geophysical Research Letters, 26*, 3029–3032.

Fliedner, M. M., & Klemperer, S. L. (2000). Crustal structure transition from oceanic arc to continental arc, Eastern Aleutian Islands and the Alaska Peninsula. *Earth and Planetary Science Letters, 179*, 567–579.

Fournelle, J.H., Marsh, B.D., & Myers, J.D. (1994). Age, character, and significance of Aleutian arc volcanism. In G. Plafker, & H.C. Berg (Eds.), *The geology of Alaska* (pp. 687–722). Geological Society of America.

Fournier, R.O. (2007). Hydrothermal systems and volcano geochemistry, chapter 10. In D. Dzurisin (Ed.), *Volcano deformation—Geodetic monitoring techniques* (pp. 323–341). Berlin: Springer-Praxis Books in Geophysical Sciences.

Fournier, T. J., & Freymueller, J. T. (2007). Transition from locked to creeping subduction in the Shumagin Region, Alaska. *Geophysical Research Letters, 34*, L06303. doi:10.1029/2006GL029073.

Fournier, T.J., Pritchard, M.E., & Riddick, S.N. (2010). Duration, magnitude, and frequency of subaerial volcano deformation events—New results from Latin America using InSAR and a global synthesis. *Geochemistry, Geophysics, and Geosystems (G^3)*, *11*, Q01003. doi: 10.1029/2009GC002558.

Freymueller, J.T., Woodard, H., Cohen, S., Cross, R., Elliott, J., Larsen, C., Hreinsdottir, S., & Zweck, C. (2008). Active deformation processes in Alaska, based on 15 years of GPS measurements. In J.T. Freymueller, P.J. Haeussler, R. Wesson, & G. Ekstrom (Eds.), *Active tectonics and seismic potential of Alaska* (Vol. 179, pp. 1–42). Washington, D.C.: AGU Geophysical Monograph, American Geophysical Union.

Geist, E. L., & Scholl, D. W. (1994). Large-scale deformation related to the collision of the Aleutian arc with Kamchatka. *Tectonics, 13*(2), 538–560.

Geist, E. L., Childs, J. R., & Scholl, D. W. (1987). Evolution and petroleum geology of Amlia and Amukta intra-arc summit basins, Aleutian Ridge. *Marine Petroleum Geology, 4*, 334–352.

Geist, E. L., Childs, J. R., & Scholl, D. W. (1988). The origin of the summit basins of the Aleutian Ridge—Implications for block rotation of an arc massif. *Tectonics, 7*, 327–342.

Gottsmann, J., & Rymer, H. (2002). Deflation during caldera unrest—Constraints on subsurface processes and hazard prediction from gravity-height data. *Bulletin of Volcanology, 64*, 338–348.

Heidbach, O., Tingay, M., Barth, A., Reinecker, J., Kurfeß, D., & Müller, B. (2008). *The world stress map database release*. Potsdam: Helmholtz Center. doi: 10.1594/GFZ.WSM.Rel2008.

Hildreth, W. (1983). The compositionally zoned eruption of 1912 in the Valley of Ten Thousand Smokes, Katmai National Park, Alaska. *Journal of Volcanology and Geothermal Research, 18*, 1–56.

Hurwitz, S., Christiansen, L., & Hsieh, P. (2007). Hydrothermal fluid flow and deformation in large calderas—Inferences from numerical simulations. *Journal of Geophysical Research, 112*, B02206. doi: 10.1029/2006JB004689.

Kay, S.M., & Kay, R.W. (1994). Aleutian magmas in space and time. In G. Plafker, & H.C. Berg (Eds.), *The geology of Alaska* (pp. 687–722). Geological Society of America.

Kay, S. M., Kay, R. W., & Citron, G. P. (1982). Tectonic controls on tholeiitic and calc-alkaline magmatism in the Aleutian arc. *Journal of Geophysical Research, 87*, 4051–4072.

Kienle, J., & Swanson, S. E. (1983). Volcanism in the eastern Aleutian Arc: late Quaternary and Holocene centers, tectonic setting and petrology. *Journal of Volcanology and Geothermal Research*, *17*, 393–432.

Lu, Z., & Wyss, M. (1996). Segmentation of the Aleutian plate boundary derived from stress direction estimates based on fault plane solutions. *Journal of Geophysical Research, 101*, 803–816.

Lu, Z., Wicks, C., Power, J., & Dzurisin, D. (2000). Ground deformation associated with the March 1996 earthquake swarm at Akutan Volcano, Alaska, revealed by satellite radar interferometry. *Journal of Geophysical Research*, *105*, 21483–21496.

Lu, Z., Power, J., McConnell, V., Wicks, C., & Dzurisin, D. (2002). Pre-eruptive inflation and surface interferometric coherence characteristics revealed by satellite radar interferometry at Makushin Volcano, Alaska, 1993–2000. *Journal of Geophysical Research*, *107*(B11), 2266, 13 pp. doi: 10.1029/2001JB000970.

Lu, Z., Masterlark, T., & Dzurisin, D. (2005). Interferometric synthetic aperture radar (InSAR) study of Okmok Volcano, Alaska, 1992–2003—Magma supply dynamics and post-emplacement lava flow deformation. *Journal of Geophysical Research*, *110*, B02403. doi: 10.1029/2004JB003148.

Lu, Z., Dzurisin, D., Wicks, C., Power, J., Kwoun, O., & Rykhus, R. (2007). Diverse deformation patterns of Aleutian volcanoes from satellite interferometric synthetic aperture radar (InSAR). In J. Eichelberger, E. Gordeev, P. Izbekov, M. Kasahara, & J. Lees (Eds.), *Volcanism and subduction—The Kamchatka Region* (Vol. 172, pp. 249–261). American Geophysical Union, Geophysical Monograph.

Lundgren, P., & Lu, Z. (2006). Inflation model of Uzon caldera Kamchatka, constrained by satellite radar interferometry observations. *Geophysical Research Letters, 33*, L06301. doi: 10.1029/2005GL025181.

Miller, T. P., & Smith, R. L. (1987). Late Quaternary caldera-forming eruptions in the Eastern Aleutian arc, Alaska. *Geology, 15*, 434–438.

Miller, T.P., McGimsey, R.G., Richter, D.H., Riehle, J.R., Nye, C.J., Yount, M.E., & Dumoulin, J.A. (1998). *Catalog of the historically active volcanoes of Alaska*. U.S. Geological Survey Open-File Report 98-582, 104 p.

Moran, S. C., Kwoun, O., Masterlark, T., & Lu, Z. (2006). On the absence of InSAR-detected volcano deformation spanning the 1995–1996 and 1999 eruptions of Shishaldin Volcano, Alaska. *Journal of Volcanology and Geothermal Research, 150*(1–3), 119–131.

Moran, S.C., Newhall, C., & Roman, D.C. (2011). Failed magmatic eruptions—Late-stage cessation of magma ascent. *Bulletin of Volcanology*, *73*(2), 115–122.

Naugler, F.P., & Wageman, J.M. (1973). Gulf of Alaska—Magnetic anomalies, fracture zones, and plate interaction. *Geological Society of America Bulletin*, *84*, 1575–1584. doi: 10.1130/0016-7606(1973)84<1575:GOAMAF>2.0.CO;2.

Neal, C.A., McGimsey, R.G., Dixon, J., & Melnikov, D. (2005). *2004 volcanic activity in Alaska and Kamchatka—Summary of events and response of the Alaska Volcano Observatory*. U.S. Geological Survey Open-File Report 2005-1308.

Newhall, C.G., & Dzurisin, D. (1988). *Historical unrest at large calderas of the world*. U.S. Geological Survey Bulletin 1855, 1108 p.

Nye, C.J. (2008). Regional variations in Aleutian magma composition (abstract). *Eos, Transactions of the American Geophysical Union*, *89*(53), 1 p.

Pavlis, G.L., Picornell, C., Serpa, L., Bruhn, R.L., & Plafker, G. (2004). Tectonic processes during oblique collision: Insights from the St. Elias orogen, northern North American Cordillera. *Tectonics*, *23*, TC3001, doi: 10.1029/2003TC001557.

Pinel, V., & Jaupart, C. (2004). Magma storage and horizontal dyke injection beneath a volcanic edifice. *Earth and Planetary Science Letters, 221*(1–4), 245–262. doi:10.1016/S0012-821X(04)00076-7.

Plafker, G. (1983). The Yakutat block—An active tectonostratigraphic terrane in Southern Alaska. *Geological Society of America Abstracts with Programs*, *15*(5), 406.

Plafker, G., Moore, J.C., & Winkler, G.R. (1994a). Geology of the Southern Alaska margin. In G. Plafker, & H.C. Berg (Eds.), *The geology of Alaska (Geology of North America, v. G-1)* (pp. 389–449). Boulder: Geological Society of America.

Plafker, G., Gilpin, L.M., & Lahr, J.C. (1994b). Neotectonic map of Alaska. In G. Plafker, & H.C. Berg (Eds.), *The geology of Alaska*. Geological Society of America, 2 sheets, scale 1:2,500,000.

Poland, M., Bawden, G., Lisowski, M., & Dzurisin, D. (2004). Newly discovered subsidence at Lassen Peak, Southern Cascade Range, California, from InSAR and GPS (abstract). *Eos, Transactions of the American Geophysical Union*, *85*(47), Fall Meeting Supplement, Abstract G51A-0068.

Poland, M., Bürgmann, R., Dzurisin, D., Lisowski, M., Masterlark, T., Owen, S., et al. (2006). Constraints on the mechanism of long-term, steady subsidence at Medicine Lake volcano, Northern California, from GPS, leveling, and InSAR. *Journal of Volcanology and Geothermal Research, 150*, 55–78. doi: 10.1016/j.volgeores.2005.07.007.

Power, J.A., Paskievitch, J.F., Richter, D.H., & McGimsey, R.G. (1996). 1996 seismicity and ground deformation at Akutan volcano, Alaska (abstract). *Eos, Transactions of the American Geophysical Union*, *77*(46, Fall Meeting Supplement), F514.

Pritchard, M.E., & Simons, M. (2002). A satellite geodetic survey of large-scale deformation of volcanic centres in the Central Andes. *Nature*, *418*, 167–171. doi: 10.1038/nature00872.

Pritchard, M.E., & Simons, M. (2004a). An InSAR-based survey of volcanic deformation in the Central Andes. *Geochemistry, Geophysics, and Geosystems (G^3)*, *5*, Q02002. doi: 10.1029/2003GC000610.

Pritchard, M. E., & Simons, M. (2004b). An InSAR-based survey of volcanic deformation in the Southern Andes. *Geophysical Research Letters, 31*, L15610. doi:10.1029/2004GL020545.

Pritchard, M. E., & Simons, M. (2004c). Surveying volcanic arcs with satellite interferometry—The Central Andes, Kamchatka, and beyond. *GSA Today, 14*(8), 4–9. doi:10.1130/1052-5173.

Ruppert, N. A., Kozyreva, N. P., & Hansen, R. A. (2012). Review of crustal seismicity in the Aleutian arc and implications for arc deformation. *Tectonophysics, 522–523*, 150–157. doi:10.1016/j.tecto.2011.11.024.

Ryan, H.F., & Scholl, D.W. (1993). Geologic implications of great interplate earthquakes along the Aleutian arc. *Journal of Gephysical Research*, *98*(B12), 22135–22146. doi: 10.1029/93JB02451.

Savage, J. C. (1983). A dislocation model of strain accumulation and release at a subduction zone. *Journal of Geophysical Research, 88*, 4984–4996.

Savage, J.C., Lisowski, M., & Prescott, W.H. (1986). Strain accumulation in the Shumagin and Yakataga seismic gaps, Alaska. *Science*, *231*(4738), 585–587. doi: 10.1126/science.231.4738.585.

Savage, J. C., Svarc, J. L., & Prescott, W. H. (1999). Deformation across the Alaska–Aleutian subduction zone near Kodiak. *Geophysical Research Letters, 26*, 2117–2120.

Scholl, D. W., Vallier, T. L., & Stevenson, A. J. (1982). Sedimentation and deformation in the Amlia fracture zone sector of the Aleutian trench. *Marine Geology, 48*, 105–134. doi:10.1016/0025-3227(82)90132-3.

Scott, W.E., Sherrod, D.R., & Gardner, C.A. (2008). Overview of the 2004 to 2006, and continuing, eruption of Mount St. Helens, Washington: chapter 1. In D.R. Sherrod, W.E. Scott, & P.H. Stauffer (Eds.), *A volcano rekindled—The renewed eruption of Mount St. Helens, 2004–2006* (pp. 3–22). U.S. Geological Survey Professional Paper 1750.

Segall, P. (2010). *Earthquake and volcano deformation* (458 pp). Princeton University Press.

Siebert, L., Simkin, T., & Kimberly, P. (2010). *Volcanoes of the world* (3rd edn., 568 p.). University of California Press and Smithsonian Institution.

Simkin, T., & Siebert, L. (2002). *Volcanoes of the world: An illustrated catalog of holocene volcanoes and their eruptions: Digital information series* (Vol. GVP-5). Washington, D.C.: Global Volcanism Program, Smithsonian Institution. http://www.volcano.si.edu/world/.

Singer, B.S., Jicha, B.R., Leeman, W.P., Rogers, N.W., Thirlwall, M.F., Ryan, Jeff, & Nicolaysen, K.E. (2007). Along-strike trace element and isotopic variation in Aleutian Island arc basalt—Subduction melts sediments and dehydrates serpentine. *Journal of Geophysical Research*, *112*(B6), 26 p. doi: 10.1029/2006JB004897.

Stern, C.R. (2004). Active Andean volcanism—Its geologic and tectonic setting. *Revista Geológica de Chile*, *31*(2), 161–206. doi: 10.4067/S0716-02082004000200001.

Tait, S., Jaupart, C., & Vergniolle, S. (1989). Pressure, gas content and eruption periodicity of a shallow, crystallizing magma chamber. *Earth and Planetary Science Letters, 92*(1), 107–123. doi: 10.1016/0012-821X(89)90025-3.

Thelen, W.A., Malone, S.D., & West, M.E. (2010). Repose time and cumulative moment magnitude: A new tool for forecasting eruptions? *Geophysical Research Letters*, *37*, L18301, 5 p. doi: 10.1029/2010GL044194.

Tregoning, P., Brunner, F. Y., Bock, Y., Puntodewo, S. S. O., McCaffrey, R., Genrich, J. F., et al. (1994). First geodetic measurement of convergence across the Java Trench. *Geophysical Research Letters, 21*(19), 2135–2138. doi: 10.1111/j.1365-246X.2007.03435.x.

Wicks, C., de la Llera, J.C., Lara, L.E., & Lowenstern, J. (2011). The role of dyking and fault control in the rapid onset of eruption at Chaitén volcano, Chile. *Nature*, *478*, 374–377. doi: 10.1038/nature10541.

Wicks, C. Jr., Dzurisin, D., Ingebritsen, S., Thatcher, W., Lu, Z., & Iverson, J. (2002). Magmatic activity beneath the quiescent Three Sisters volcanic center, central Oregon Cascade Range, USA. *Geophysical Research Letters*, *29*(7), 26-1–26-4. doi: 10.1029/2001GL014205.

Wicks, C, Jr, Thatcher, W., & Dzurisin, D. (1998). Migration of fluids beneath Yellowstone caldera inferred from satellite radar interferometry. *Science, 282*, 458–462.

Worrall, D.M. (1991). Tectonic history of the Bering Sea and the evolution of tertiary strike-slip basins of the Bering Shelf. *Geological Society of America Special Paper*, *257*, 120 p.